Available online at www.sciencedirect.com
ScienceDirect
Catalysis Today 126 (2007) 96–102
CATALYSIS TODAY
www.elsevier.com/locate/cattod

# Combining theoretical description with experimental *in situ* studies on the effect of potassium on the structure and reactivity of titania-supported vanadium oxide catalyst

H. Si-Ahmed [a], M. Calatayud [a], C. Minot [a], E. Lozano Diz [b], A.E. Lewandowska [b], M.A. Bañares [b,*]

[a] *Université Pierre et Marie Curie-Paris6, UMR CNRS 7616 LCT, Paris F-75005, France*
[b] *Instituto de Catálisis y Petroleoquímica, CSIC, Marie Curie, 2, E-28049 Madrid, Spain*

Available online 19 April 2007

**Abstract**

The influence of potassium on the structure and properties of titania-supported vanadium oxide catalysts has been studied by DFT calculations and measured experimentally by *in situ* temperature-programmed Raman (TP-Raman) spectroscopy and temperature-programmed reduction (TPR). Below monolayer coverage, potassium coordinates to surface vanadium oxide species altering its structure but it does not form bulk compounds. Theory and experiments agree on the weakening of the terminal V=O bond due to the interaction between potassium and vanadium oxide. K-doped vanadia–titania catalysts show a decrease of reducibility with K loading in line with the decrease in the calculated hydrogen adsorption energy for K-doped models.


*Keywords:* Vanadium oxide; Catalyst; Raman spectroscopy

## 1. Introduction

The oxidative dehydrogenation (ODH) of light alkanes to alkenes possesses great industrial relevance and it has extensively been studied [1–8]. Vanadium oxide is present in most of the catalysts for selective oxidation of alkanes, which afford high productivity and high yield at low temperatures. A rational catalysts design requires detailed information on the nature of the active sites and their role in the catalytic cycle. The catalytic properties of supported vanadia for selective oxidation reactions are strongly influenced by the preparation method, nature of the support and of the promoter. Alkali metals, in particular potassium, are often mentioned as promoters for industrial catalysts since they afford higher selectivity for partial oxidation reactions [9–23].

The molecular structure of supported vanadium oxides has been studied by different experimental approaches [24–26]; in particular, the interaction between supported vanadia and the oxide support (e.g., titania) has been studied in detail by several techniques [27–30]. The use of calculations provides models to describe the structure, spectrum characteristics and reactivity [31–36]. The interactions of alkali cations (e.g. potassium, etc.), with oxide supports (e.g. titania, etc.) have been extensively studied by several experimental techniques [10,19,40] as well as theoretical calculations [37–39]. However, the role of alkali dopants on the structure and properties of supported vanadia is not fully understood. Titania-supported vanadia shows a strong dependence on the sequence of preparation so that V oxide on K-doped titania appears to cover K sites and the molecular structures of vanadia resemble those of surface vanadia [11,40,9,41]. At low coverage, the presence of K does not lead to the formation of vanadates, but its interaction with surface vanadia results in weaker V=O bonds in the surface vanadia species [10,19,40].

This work aims to provide a molecular description of the structure and reactivity of titania-supported vanadium oxide and the relevance of alkali doping, by a complementary experimental and theoretical approach. Undoped and K-doped $VO_x/TiO_2$ catalysts have been prepared and characterized by *in situ* Raman spectroscopy, temperature-programmed reduction

* Corresponding author. Tel.: +34 91 585 4788; fax: +34 91 585 4760.
*E-mail address:* CATTOD.banares@icp.csic.es (M.A. Bañares).

0920-5861/$ – see front matter 
doi:10.1016/j.cattod.2007.03.003

(TPR); the structural and reactive features are contrasted with those described by DFT calculations. The results obtained will be of great importance in understanding the events taking place in catalytic materials under reaction conditions and is thus a complementary tool to describe the structures and performances observed in *operando* studies.

## 2. Experimental

### 2.1. Preparation of samples

The catalysts were prepared by sequential impregnation of titanium (IV) oxide (*Alfa Aesar*, 100% anatase, $S_{BET}$ = 166 $m^2/g$). At the beginning $TiO_2$ was modified by potassium. The K-doped catalysts were prepared from aqueous solution of potassium hydroxide (*Panreac*, 90%). The suspension was evaporated in rotatory evaporator at 338 K. After drying the samples were calcined at 723 K for 4 h in air. The rate of the heating was 5 K $min^{-1}$. Vanadia on titania and K-doped titania materials were prepared from an aqueous solution of ammonium metavanadate (*Sigma*, 99.99%). Oxalic acid (*Panreac*, 99.5%) was added to an aqueous solution of $NH_4VO_3$ to facilitate dissolving the salts. The solution was kept under stirring at 323 K for 50 min. The resulting solid was dried and calcined at the same conditions like K-doped samples. The amount of V corresponds to half monolayer coverage 4 atoms/$nm^2$ (9.1 wt.%). Concentration of $K_2O$ was calculated to 0.4, 0.8, 1.5 and 2.3 wt.%, which correspond to a K/V atomic ratio of 0.075, 0.15, 0.30 and 0.45, respectively. Catalysts are labeled as $x$V/$y$K/$TiO_2$, where $x$ and $y$ indicate the number of atoms per square nanometer of V and K, respectively.

### 2.2. Raman

Raman spectra were run with a single monochromator *Renishaw* System-1000 microscope Raman equipped with a cooled CCD detector (200 K) and holographic super-Notch filter. The holographic Notch filter removes the elastic scattering while the Raman signal remains high. The powder samples were excited with the 514 nm $Ar^+$ line; spectral resolution was near 3 $cm^{-1}$ and spectrum acquisition consisted of 20 accumulations of 10 s. The spectra were obtained under dehydrated conditions in a hot stage (*Linkam* TS-1500). The samples were dehydrated in synthetic airflow at 673 K for 1 h. The rate of the heating was 5 K $min^{-1}$. The spectra of hydrated samples were obtained at room temperature in a flow of humid air.

### 2.3. $H_2$-TPR

Temperature-programmed reduction was performed in a fixed-bed quartz reactor with a Micromeritics TPD/TPR 2900 analyzer equipped with a thermal conductivity detector (TCD). The reduction of the samples was carried out using $H_2$/Ar (10 vol.%) as reductant (flow rate = 40 $cm^3$ $min^{-1}$). A 30 mg of the samples placed in the reactor were activated in a flow of synthetic air at 673 K at a rate of 5 K $min^{-1}$. Subsequently the sample was cooled to RT in synthetic air, then, it was heated at a rate of 10 K $min^{-1}$ to 1223 K under the reductant mixture. The water produced during the reduction was condensed in a cold trap dipped in a mixture of isopropanol and liquid nitrogen.

### 2.4. Computational details

The DFT calculations have been performed at the B3LYP/6-31G* level with the Gaussian 03 code [42]. Structures were first optimized and then vibrational frequencies were analytically computed at the stationary point. The Raman intensity has been computed by numerical differentiation of dipole derivatives with respect to the electric field as implemented in the code. This method has proven to be accurate enough to obtain a good description of the structure and vibrational spectrum of $V_xO_y$ gas-phase clusters [43].

The catalyst active phase is modeled by a $V_2O_5$ cluster. This simple system accounts for the basic features of reactivity in vanadia catalysts and has been studied both experimentally and theoretically [31,44–47]. The surfaces of the bulk transition metal oxide have been described as a collection of clusters; this allows for localized bonding models to be used to study surfaces [48]. The structure contains a VOVO cycle terminated by three vanadyl V=O bonds with V=O distances of 1.58 Å. One vanadium atom is three-fold coordinated, the other is four-fold coordinated. The interaction with potassium is modeled by considering the formal adsorption of a KOH unit: the $OH^-$ group binds to the undercoordinated vanadium and the K atom to two vanadyl bonds. The K/V ratio is in our model 0.5 which is very close to the experimental sample 4V/1.8K/$TiO_2$. Several starting points have been considered; the best model is shown in Fig. 1. In this model the K atom is in the vicinity of two V=O bonds, with K–O distances of 2.63–2.72 Å, and one oxygen of the cycle at almost 4 Å. The main effect on the catalyst is to elongate the vanadyl bonds in interaction with the alkali atom, which pass from 1.58 to 1.62 Å.

The adsorption of hydrogen has been calculated in order to investigate the effect in reducibility. We report the adsorption energy of one and two hydrogen atoms on the bare and doped models. The adsorption energy is defined as follows:

$$E_{ads}(H) = \frac{E_{nH-xV_2O_5} - nE_H - E_{xV_2O_5}}{n}$$

where $E$ are the total energy of the system without ($xV_2O_5$) and with hydrogen ($n$H–$xV_2O_5$), for $n$ atoms of hydrogen. Negative values indicate exothermic processes. The hydrogenated systems are open-shell and spin-unrestricted wavefunctions are used, with no spin contamination in any case.

## 3. Results and discussion

The Raman spectra of K-free and K-doped titania-supported vanadium oxide species are dominated by the Raman features of titanium oxide (not shown). The bands at 638, 519 and 394 $cm^{-1}$ are assigned to anatase polymorphic form [49]. The absence of the bands at 830 and 450 $cm^{-1}$ allows excluding the presence of rutile phase in the support oxide. The anatase bands

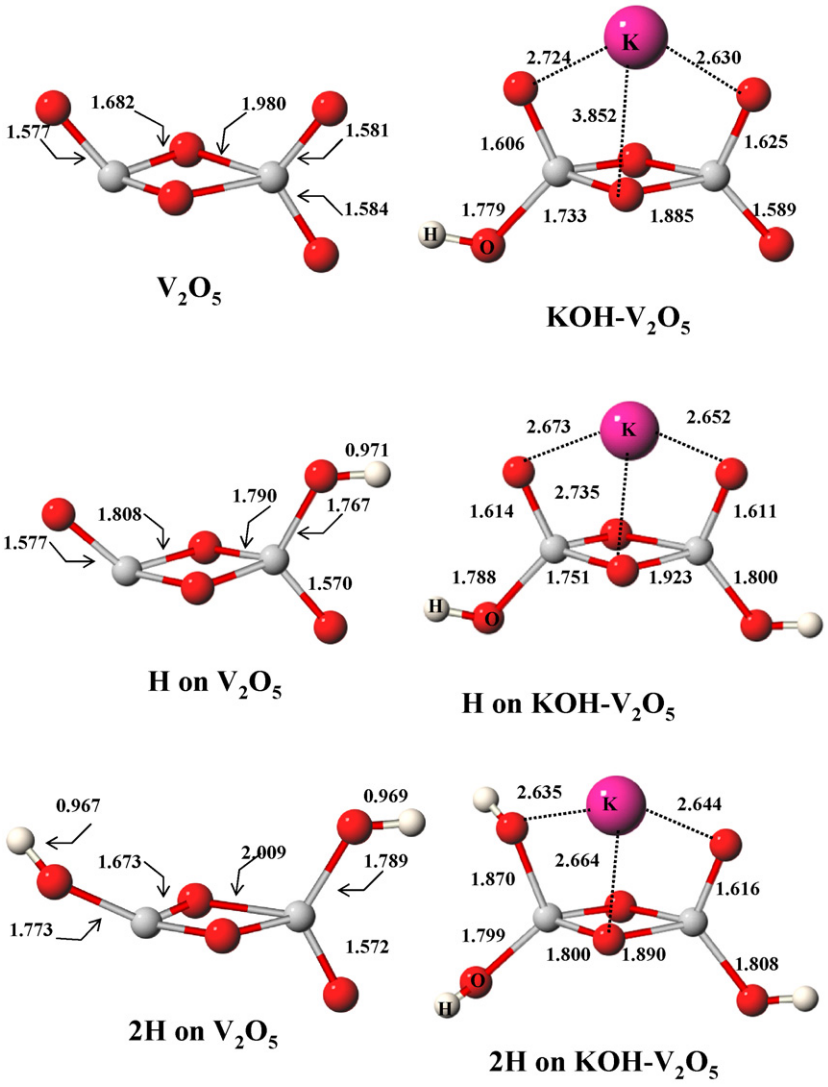


Fig. 1. Computational models for the bare catalyst $V_2O_5$ (left) and K-doped KOH–$V_2O_5$ (right). The best hydrogenated systems are shown. Distances in Å.

overlap the surface vanadium oxide species Raman features below 750 $cm^{-1}$. Spectra of the dehydrated vanadium catalysts are presented in the range from 1100 to 700 $cm^{-1}$ in Fig. 2.

The Raman spectrum of dehydrated 4V/$TiO_2$ catalyst is shown in Fig. 2Aa. The band at 1032 $cm^{-1}$ is attributed to V=O stretching mode of isolated monovanadates species [50–55]. The band at ~924 $cm^{-1}$ is related to the V–O–V functionalities of the polymeric species in the form of polyvanadate domains or chains [49–51]. The titania-supported vanadia catalyst exhibits both isolated tetrahedral as well as a polymeric vanadium oxide species. The Raman band at 994 $cm^{-1}$ is assigned to crystalline $V_2O_5$, whose Raman section is ca. 20 times that of surface vanadia species [56]. The low intensity of this band suggests that the amount of crystalline vanadium oxide is not high and that it is in the form of nanocrystalline particles. The dehydrated spectra of K-doped samples exhibit a band assigned to the V=O stretching vibration (Fig. 2Ab–e). The presence of potassium affects the position of this band. An increase of potassium content monotonically shifts V=O band towards lower wavenumbers: from 1032 $cm^{-1}$ (K-free sample, Fig. 2Aa) to 988 $cm^{-1}$ in 4V/1.8K/$TiO_2$ (1.8 K atoms/$nm^2$, Fig. 2Ae). The interaction between vanadium and potassium also influences the intensity of the Raman bands. They are broader and weaker in comparison with the band of 4V/$TiO_2$, which suggests a broader distribution of states. The K-doped catalysts do not exhibit the Raman band of V–O–V functionalities. This phenomenon can result from the shifting of the Raman band towards wavenumber dominated by the support bands or reflect a decrease in the polymerization degree of the surface vanadium oxide species. As potassium loading increases, a broad Raman band near 770 $cm^{-1}$ becomes increasingly important and shifts to 830 $cm^{-1}$, when a new Raman band becomes evident at 870 $cm^{-1}$. Potassium metavanadate ($KVO_3$) exhibits its most intense Raman band at 932 $cm^{-1}$, potassium divanadate ($K_4V_2O_7$) and potassium orthovanadate ($K_3VO_4$) exhibit their most intense Raman band at 868 $cm^{-1}$ [57]. In particular, potassium orthovanadate possesses an intense Raman band at 867 $cm^{-1}$ and weaker ones at 818 and 760 $cm^{-1}$ [57]. Therefore, as K loading increases (increases in K/V atomic ratio) surface vanadium species are

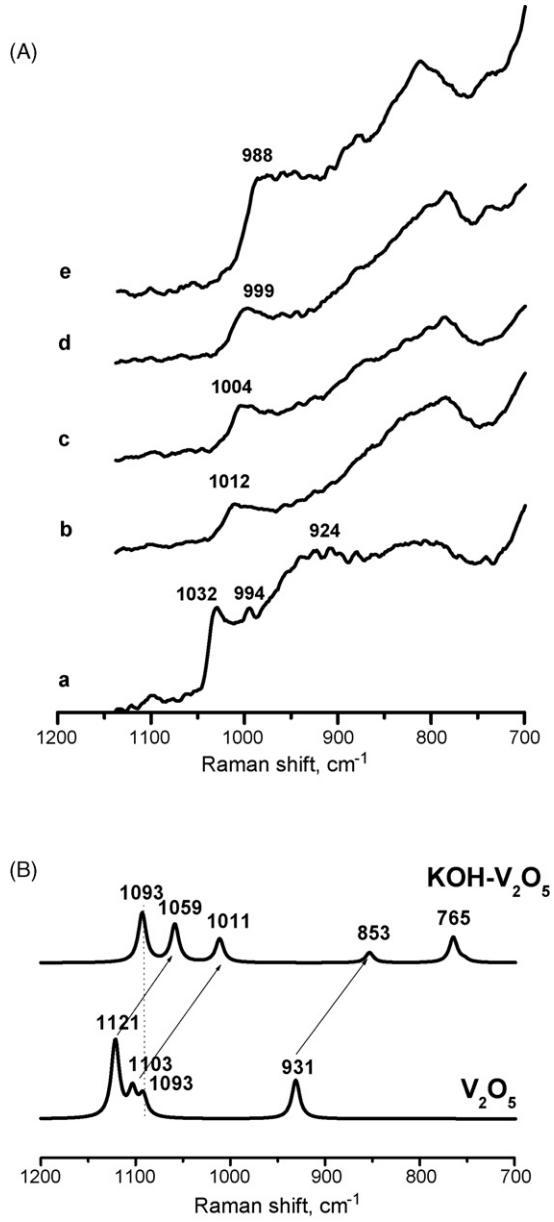


Fig. 2. (A, top) Raman spectra of dehydrated titania-supported oxides at 323 K: (a) 4V/$TiO_2$; (b) 4V/0.3K/$TiO_2$; (c) 4V/0.6K/$TiO_2$; (d) 4V/1.2K/$TiO_2$; (e) 4V/1.8K/$TiO_2$. (B, bottom) Calculated Raman spectra for the $V_2O_5$ and KOH–$V_2O_5$ models.

increasingly affected upon K–V interaction and some incipient aggregation into incipient bulk potassium vanadate crystalline phases becomes apparent.

The calculated Raman spectrum of the $V_2O_5$ cluster shows the basic features of the vanadia-based catalyst: the vanadyl stretching bands around 1100 $cm^{-1}$ and the V–O–V stretching at 930 $cm^{-1}$ (Fig. 2B). Note that the absolute values, especially for high frequencies, are overestimated in DFT; we focus here in the comparison between the bare and the K-doped frequency shifts rather than on the reproduction of numerical values. Since in the bare model there are three inequivalent V=O, three vanadyl bands appear in the calculated spectrum. Upon interaction with K two of them elongate and consequently the bands are shifted towards lower wavenumbers. A finer analysis of the clusters spectra can be done by considering the vibrational modes associated to each frequency: the band at 1121 $cm^{-1}$ for the bare system is assigned to the O=V V=O symmetric stretching, it is displaced to 1059 $cm^{-1}$ (redshifted by 63 $cm^{-1}$) in the K-doped series. The band at 1103 $cm^{-1}$ is assigned to O=V=O asymmetric stretching and is shifted to 1011 $cm^{-1}$ (redshifted by 92 $cm^{-1}$) in the K-doped series. The V=O which is not in interaction with K vibrates at 1093 $cm^{-1}$ and remains basically unchanged in the bare cluster. The average displacement for the three vanadyl bonds is then of 50 $cm^{-1}$, which is in agreement with the experimental value of 45 $cm^{-1}$. The calculated spectrum also accounts for the decrease in activity and the broadening of the vanadyl band as found in the experiment. The lower band at 931 $cm^{-1}$ corresponds to the symmetric O–V–O stretching of the cycle, it shifts to 853 $cm^{-1}$ (−78 $cm^{-1}$) and decreases in intensity as in the experiment. Finally, the band appearing at 765 $cm^{-1}$ is associated to the V–OH stretching, not present in the bare model.

Fig. 3 illustrates the $H_2$-TPR profiles of the carrier titanium oxide (dashed lines) and those corresponding to titania-supported catalysts (solid lines). The temperature of peaks maxima relate to the support reduction ($T_{M\text{-}Si}$) and the vanadia species reduction ($T_{M\text{-}Vi}$) are summarized in Table 1. $TiO_2$ is a reducible oxide support. The TPR profile of titania shows three small reduction peaks with maxima at 591, 688 and 774 K. Above 1040 K the $H_2$ consumption rises gradually with temperature. This trend is consistent with those reported in

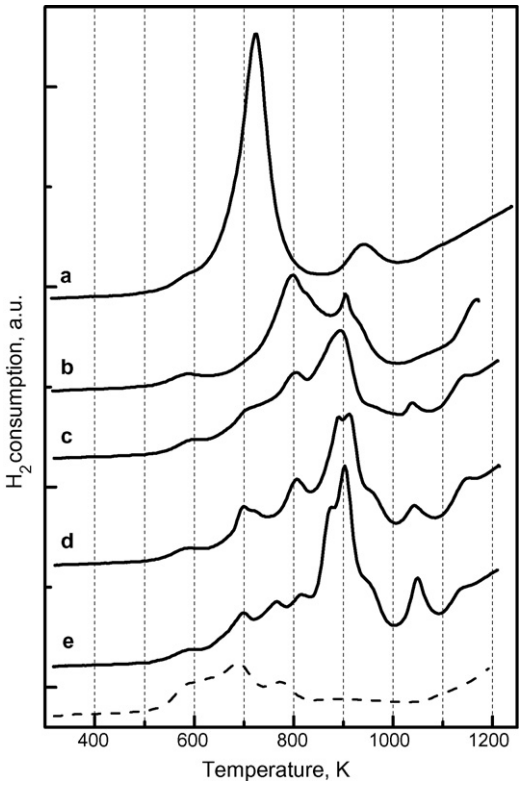


Fig. 3. $H_2$-TPR profiles of titania-supported catalysts: (a) 4V/$TiO_2$; (b) 4V/0.3K/$TiO_2$; (c) 4V/0.6K/$TiO_2$; (d) 4V/1.2K/$TiO_2$; (e) 4V/1.8K/$TiO_2$. The profile marked by dash line describes the reduction of $TiO_2$.

Table 1
The reduction temperatures ($H_2$-TPR) of the titania-supported catalysts

| Catalyst | Support $T_{red}$ (K) | | | Vanadia $T_{red}$ (K) | | | | |
|---|---|---|---|---|---|---|---|---|
| | $T_{M\text{-}S1}$ | $T_{M\text{-}S2}$ | $T_{M\text{-}S3}$ | $T_{M\text{-}V1}$ | $T_{M\text{-}V2}$ | $T_{M\text{-}V3}$ | $T_{M\text{-}V4}$ | $T_{M\text{-}V5}$ |
| $4V/TiO_2$ | 588 | | | 724 | | 941 | | |
| $4V/0.3K/TiO_2$ | 588 | | | 799 | | 904 | | |
| $4V/0.6K/TiO_2$ | 590 | 717 | | 805 | 874 | 895 | | 1039 |
| $4V/1.2K/TiO_2$ | 590 | 700 | | 807 | 890 | 911 | | 1042 |
| $4V/1.8K/TiO_2$ | 588 | 699 | 766 | 816 | 877 | 903 | | 1050 |
| $TiO_2$ | 591 | 688 | 774 | | | | | |
| $V_2O_5$ | | | | 575 | | 945 | 979 | 1064 |

literature [58,59]. It should be noted that the reduction profile for $TiO_2$ reported in the literature differs in the temperature and number of the reduction peaks. However, the intrinsic reducibility of the support oxides appears to depend on the morphological properties and impurities [58]. The reduction profiles for the vanadia catalysts exhibit maxima at lower temperature related to the reduction of titanium oxide (Table 1). The TPR profile of $4V/TiO_2$ catalyst exhibits one sharp maximum at 724 K ($T_{M\text{-}V1}$) and smaller one at 941 K ($T_{M\text{-}V3}$) (Fig. 3a). According to the literature [52,59,60], the maximum at ~750 K is assigned to the reduction of monomeric vanadium oxide species. It was reported that increasing vanadia loading on titania shifts the TPR peak to higher temperature [52,60]. This trend indicated that the reduction of polymeric vanadia species is more difficult compared to the monomeric ones on titania. The first reduction peak can thus be attributed to the reduction of monomeric and polymeric vanadium oxide species. At intermediate vanadium loading both of these species exist on titania surface. The existence of these species in $4V/TiO_2$ sample was confirmed by Raman spectroscopy. The reduction profile of $4V/0.3K/TiO_2$ catalyst, the one with lowest potassium content, shows two reduction peaks (Fig. 3b). The maximum at 799 K is assigned to reduction of surface vanadium oxide species. The reduction maximum corresponding to monomeric species shifts to higher temperature and decreases intensity with an increasing of potassium content (Fig. 3b–e).

The peak at 904 K appears at lower temperature than the peak associated to the reduction of bulk-like species in the K-free sample (Table 1), and exhibits a sharper profile. K loading makes this reduction peak increasingly important (Fig. 3c–e). It is likely, that the reduction maxima near 900 K correspond to K-modified V oxide species. TPR profiles of K-doped materials exhibit shoulders at ~870 K ($T_{M\text{-}V2}$), which can be attributed to vanadium oxide in the other interaction with potassium, probably at different stoichiometries, depending on K/V atomic ratio. The new reduction peak near 1050 K becomes increasingly important with potassium loading, its intensity growth runs parallel to the formation of incipient potassium orthovanadate, revealed by Raman spectra.

To understand the relevance of potassium on the reduction profiles of titania-supported vanadium oxide species, the adsorption of one and two hydrogen atoms on the bare and doped models has been calculated. The addition of H has been done on the vanadyl V=O bonds, the most favorable structures are shown in Fig. 1. The adsorption energy for such processes is reported in Table 2. The adsorption of hydrogen is exothermic in all cases, more favorable for bare model than for the K-doped system: for $V_2O_5$, the heat of adsorption for one H is −4.08 eV, −2.94 eV for the doped system. The adsorption of a second H atom is favorable by −2.59 eV for the bare, −2.33 eV for the doped system. The effect of K would then be to decrease reducibility. This is also observed in the experimental TPR temperatures that increase the reduction temperature values with K loading.

The interaction of hydrogen with the catalyst oxygen leads to the formation of a strong OH bond and the reduction of the vanadium atoms:

$$H \rightarrow H^+ + 1e^-$$

$$V^{5+} + 1e^- \rightarrow V^{4+}$$

$$O_{surf}{}^{2-} + H^+ \rightarrow O_{surf}H^-$$

$$H + V^{5+} + O_{surf}{}^{2-} \rightarrow V^{4+} + O_{surf}H^-$$

Since the formation of a hydroxyl bond is comparable in the undoped and doped systems, the difference in the adsorption energy comes from the reducibility. Indeed, the undoped model presents a HOMO–LUMO gap of 2.90 eV, while in the case of K-doped it is of 4.43 eV. The wide gap is a consequence of the interaction K–O that stabilizes the levels of the oxygen sites involved. The electron transfer is facilitated by low LUMO levels coming from the vanadium sites. Thus, upon one H adsorption the electron is transferred to the vanadium three-fold coordinated, as confirmed by an analysis of the spin density. The same vanadium captures the electron for the K-doped system. The adsorption of a second H leads to two unpaired

Table 2
Calculated values for the hydrogen adsorption on bare and K-doped models, in eV

| System | $E_{ads}$ | | Average |
|---|---|---|---|
| | First H | Second H | |
| $V_2O_5$ | −4.08 | −2.59 | −3.33 |
| $KOH–V_2O_5$ | −2.94 | −2.33 | −2.63 |

All the values are exothermic.

electrons, one on each vanadium, this situation is preferred to a singlet closed-shell configuration. The formal oxidation state cannot be determined from DFT calculations due to the delocalized description of the charge density in this methodology. The addition of a second hydrogen is less favorable due to the fact that the vanadium atom is already reduced.

In summary, the nature of surface vanadium oxide species is affected by the presence of potassium. This is evident in the reducibility and in the Raman spectra, which are in agreement with DFT calculations. The Raman spectra evidence an alteration in the nature of surface vanadium oxide species by K. Potassium interacts with surface vanadium oxide species, giving rise to V–O–K and Ti–O–K linkages; such scenario has been proposed for K-doped alumina-supported vanadia [61]. It has been described how the Raman bands of surface vanadia species increasingly change with potassium content [40]. $^{51}$V NMR-MAS spectra show that the potassium addition strongly changes the environment of V sites and forms alkali vanadates on V/$TiO_2$ [11,62,63] or bronzes [11,62,15,64]. Our results show the incipient formation of bulk V–K–O compounds (polymorphic potassium vanadates) at the highest V + K loading on titania. The main feature of the K-modified surface vanadia appears to be a weakening of the terminal V=O bond and the development of a Raman band near 800 $cm^{-1}$ associated to the V–K–O system. The TPR profiles show that the interaction between surface vanadia and surface K oxides decreases the reducibility of the surface vanadium oxide species. Structural and reducibility dependence on K loading are in agreement with DFT results. Therefore, for the hydrogenation the changes in the strength of the terminal V=O bond does not correlate with change in reducibility.

## 4. Conclusion

The combination of theoretical calculations with experimental studies provides a more accurate description of the catalyst structure and reactivity towards different molecules, which can be contrasted with experimental data. This fundamental knowledge is critical to assess structure–activity relationships at a molecular scale, and will significantly contribute to understand *in situ* and *operando* studies of catalytic materials at work. In this paper, DFT calculations and experimental data provide complementary information on the changes on the structure and reactivity that directly connect to the identification of active sites. DFT calculations show that the potassium presence on $V_2O_5$ weakens the terminal V=O bond, which should redshift by ca. 50 $cm^{-1}$. The model also describes how potassium addition makes less favorable the interaction with hydrogen, thus decreasing the reducibility of vanadia sites. The experimental data are in agreement with theoretical calculations. Raman spectra show that potassium loading increasingly weakens the terminal V=O bond in $VO_x$/$TiO_2$ catalysts. As K loading increases, such K–V interaction leads to the incipient formation of bulk potassium vanadates. The $H_2$-TPR profiles show a decrease of reducibility with potassium content. Therefore, for the hydrogenation the changes in the strength of the terminal V=O bond does not correlate with change in reducibility. These trends cannot be understood if the terminal V=O bond is the active site of vanadia species, since this bond becomes more labile upon interaction with potassium.

## Acknowledgements

This work has been supported by the COST ACTION D36 (Working Group D36-006-06) and has been accomplished in the frame of the French GDR ‘‘Dynamique moléculaire quantique appliqué à la catalyse’’. Computational facilities by CCRE and IDRIS are acknowledged. Support was provided by the Spanish Ministry of Education and Science CTQ2005-02802/PPQ. AEL acknowledges Spanish Ministry of Education and Science for a postdoctoral fellowship (SAB2003-0179), and ELD acknowledges Comunidad de Madrid project for a contract.

## References

[1] H.H. Kung, Adv. Catal. 40 (1994) 1.
[2] S. Albonetti, F. Cavani, F. Trifirò, Catal. Rev. Sci. Eng. 38 (4) (1996) 413.
[3] M.A. Bañares, Catal. Today 51 (1999) 319.
[4] A. Khodakov, B. Olthof, A.T. Bell, E. Iglesia, J. Catal. 181 (1999) 205.
[5] K. Chen, E. Iglesia, A.T. Bell, J. Catal. 192 (2000) 197.
[6] T. Blasco, J.M. López Nieto, Appl. Catal. 157 (1997) 117.
[7] J.C. Védrine, Stud. Surf. Sci. Catal. 110 (1997) 61.
[8] E. Heracleous, M. Machli, A. Lemonidou, I. Vasalos, J. Mol. Catal. A 232 (2005) 29.
[9] G. Deo, I.E. Wachs, J. Catal. 146 (1994) 335.
[10] L. Lietti, P. Forzatti, G. Ramis, G. Busca, F. Bregani, Appl. Catal. 3 (1993) 13.
[11] D. Courcot, A. Ponchel, B. Grzybowska, Y. Barbaux, M. Rigole, M. Guelton, J.P. Bonnelle, Catal. Today 33 (1997) 109.
[12] G. Martra, F. Arena, S. Coluccia, F. Frusteri, A. Parmaliana, Catal. Today 63 (2000) 197.
[13] M.L. Ferreira, M. Volpe, J. Mol. Catal. 164 (2000) 281.
[14] A. Lemonidou, L. Nalbandian, I.A. Vasalos, Catal. Today 61 (2000) 333.
[15] T. Ono, Y. Tanaka, T. Takeuchi, K. Yamamoto, J. Mol. Catal. 159 (2000) 293.
[16] L. Kiwi-Minsker, D.A. Bulushev, F. Rainone, A. Renken, J. Mol. Catal. 184 (1/2) (2002) 223–235.
[17] J.M. López Nieto, P. Concepción, A. Dejoz, F. Melo, H. Knözinger, M.I. Vázquez, Catal. Today 61 (2000) 361.
[18] C. Resini, M. Panizza, L. Arrighi, S. Sechi, G. Busca, R. Miglio, S. Rossini, Chem. Eng. J. 89 (2002) 75.
[19] L. Kiwi-Minsker, D.A. Bulushev, F. Rainone, A. Renken, J. Mol. Catal. 184 (2002) 223.
[20] A. Klisińska, K. Samson, I. Gressel, B. Grzybowska, Appl. Catal. A: Gen. 309 (2006) 10.
[21] A. Klisińska, S. Loridant, B. Grzybowska, J. Stoch, I. Gressel, Appl. Catal. A: Gen. 309 (2006) 17.
[22] Z. Zhao, J. Liu, A. Duan, C. Xu, T. Kobayashi, I.E. Wachs, Top. Catal. 38 (2006) 309.
[23] M. De, D. Kunzru, Catal. Lett. 102 (2005) 237.
[24] H.-J. Freund, Catal. Today 100 (2005) 3.
[25] A. Brückner, Catal. Rev. 45 (2003) 97.
[26] J.M. Tatibouët, Appl. Catal. A: Gen. 148 (1997) 213.
[27] Ramis, Gianguido, G. Busca, F. Bregani, P. Forzatti, Appl. Catal. 64 (1990) 259–278.
[28] B. Grzybowska-Świerkosz, Appl. Catal. A: Gen. 157 (1997) 263.
[29] N.-Y. Topsoe, Science 265 (1994) 1217.
[30] M.D. Amiridis, I.E. Wachs, G. Deo, J.-M. Jehng, D.S. Kim, J. Catal. 161 (1996) 247.
[31] M. Calatayud, A. Beltran, et al. J. Phys. Chem. A 105 (2001) 9760.

[32] M. Calatayud, B. Mguig, C. Minot, Surf. Sci. Rep. 55 (2004) 169.
[33] O.L.J. Gijzeman, J.N.J. van Lingen, J.H. van Lenthe, S.J. Tinnemans, D.E. Keller, B.M. Weckhuysen, Chem. Phys. Lett. 397 (2004) 277.
[34] M. Calatayud, C. Minot, J. Phys. Chem. B 108 (2004) 15679.
[35] A. Klisinska, A. Hara, K. Samson, M. Witko, B. Grzybowska, J. Mol. Catal. A 210 (2004) 87.
[36] N. Magg, B. Immaraporn, J.B. Giorgi, T. Schroeder, M. Bäumer, J. Döbler, Z. Wu, E. Kondratenko, M. Cherian, M. Baerns, P.C. Stair, J. Sauer, H.-J. Freund, J. Catal. 226 (2004) 88.
[37] T. Bredow, E. Aprà, M. Catti, G. Pacchioni, Surf. Sci. 418 (1998) 150.
[38] J. Muscat, N.M. Harrison, G. Thornton, Phys. Rev. B 59 (1999) 15457.
[39] M.A. San Miguel, C.J. Calzado, J.F. Sanz, J. Phys. Chem. B 105 (2001) 1794.
[40] G.G. Cortez, J.L.G. Fierro, M.A. Bañares, Catal. Today 78 (2003) 219.
[41] C. Resini, T. Montanari, G. Busca, J.M. Jehng, I.E. Wachs, 99 (2005) 105.
[42] M.J. Frisch, G.W. Trucks, et al., Gaussian 03 (Revision A.1), Gaussian, Inc., Pittsburgh, PA, 2003.
[43] M. Calatayud, A. Beltran, et al. J. Phys. Chem. A 105 (2001) 9760–9775.
[44] K.R. Asmis, G. Meijer, et al. J. Chem. Phys. 120 (2004) 6461.
[45] Y. Matsuda, E.R. Bernstein, J. Phys. Chem. A 109 (2005) 3803–3811.
[46] S.F. Vyboishchikov, J. Sauer, J. Phys. Chem. A 105 (2001) 8588–8598.
[47] K.A. Zemski, D.R. Justes, et al. J. Phys. Chem. B 106 (2002) 6136–6148.
[48] G.A. Somorjai, Introduction to Surface Chemistry and Catalysis, John Wiley & Sons, New York, 1994.
[49] G.T. Went, S.T. Oyama, A.T. Bell, J. Phys. Chem. 94 (1990) 4240.
[50] M.A. Bañares, I.E. Wachs, J. Raman Spectrosc. 33 (2002) 259.
[51] A. Christodoulakis, M. Machli, A.A. Lemonidou, S. Boghosian, J. Catal. 222 (2004) 293.
[52] D.A. Bulushev, L. Kiwi-Minsker, F. Rainone, A. Renken, J. Catal. 205 (2002) 115.
[53] S. Besselmann, E. Löffler, M. Muhler, J. Mol. Catal. A: Chem. 162 (2000) 401.
[54] M.A. Vuurman, I.E. Wachs, A.M. Hirt, J. Phys. Chem. 95 (1991) 9928.
[55] T. Machej, J. Haber, A.M. Turek, I.E. Wachs, Appl. Catal. 70 (1991) 115.
[56] S. Xie, E. Iglesia, A.T. Bell, Langmuir 16 (2000) 7162.
[57] RASMIN, Raman Spectra Database of Minerals and Inorganic Materials, National Institute for Advanced Industrial Science and Technology, Japan (http://www.aist.go.jp/RIODB/rasmin/E_index.htm).
[58] F. Arena, F. Frusteri, A. Parmaliana, Appl. Catal. A: Gen. 176 (1999) 189.
[59] F. Arena, N. Giordano, A. Parmaliana, J. Catal. 167 (1997) 66.
[60] S. Besselmann, C. Freitag, O. Hinrichsen, M. Muhler, Phys. Chem. Chem. Phys. 3 (2001) 4633.
[61] G. Ramis, G. Busca, F. Bregani, Catal. Lett. 18 (1993) 299.
[62] D.A. Bulushev, L. Kiwi-Minsker, V.I. Zaikovskii, O.B. Lapina, A.A. Ivanov, S.I. Reshetnikov, A. Renken, Appl. Catal. 202 (2000) 243.
[63] D.A. Bulushev, F. Rainone, L. Kiwi-Minsker, A. Renken, Langmuir 17 (2001) 5276.
[64] A. Brückner, U. Bentrup, A. Martin, J. Radnik, L. Wilde, G.-U. Wolf, Stud. Surf. Sci. Catal. 130 (2000) 359.